

Synthesis and Characterization of the Novel Monoamide Derivatives of Gd–TTDA

Yun-Ming Wang,^{*†} Cha-Ru Li,[†] Yu-Chin Huang,[†] Ming-Hung Ou,^{†‡} and Gin-Chung Liu[§]

Faculty of Medicinal and Applied Chemistry, Graduate Institute of Pharmaceutical Sciences, and Department of Medical Imaging, Kaohsiung Medical University, 100 Shih-Chuan 1st Road, Kaohsiung, 807 Taiwan, Republic of China

Received May 7, 2004

For this study, the *N*-monoamide derivatives of TTDA (3,6,10-tri(carboxymethyl)-3,6,10-triazadodecanedioic acid), *N*-methylamide (TTDA-MA), *N*-benzylamide (TTDA-BA), and *N*-2-methoxybenzylamide (TTDA-MOBA), were synthesized. Their protonation constants and stability constants ($\log K_{ML}$'s) formed with Ca^{2+} , Zn^{2+} , Cu^{2+} , and Gd^{3+} were determined by potentiometric titration in 0.10 M Me_4NCl at 25.0 ± 0.1 °C. The relaxivity values of $[\text{Gd}(\text{TTDA-MA})]^-$, $[\text{Gd}(\text{TTDA-BA})]^-$, and $[\text{Gd}(\text{TTDA-MOBA})]^-$ remained constant with respect to pH changes over the range 4.5–12.0. The ^{17}O NMR chemical shift of H_2O induced by $[\text{Dy}(\text{TTDA-MA})(\text{H}_2\text{O})]^-$ at pH 6.80 showed 0.9 inner-sphere water molecules. Water proton relaxivity values for $[\text{Gd}(\text{TTDA-MA})(\text{H}_2\text{O})]^-$, $[\text{Gd}(\text{TTDA-BA})(\text{H}_2\text{O})]^-$, and $[\text{Gd}(\text{TTDA-MOBA})(\text{H}_2\text{O})]^-$ at 37.0 ± 0.1 °C and 20 MHz are 3.89, 4.21, and 4.25, respectively. The water-exchange lifetime (τ_M) and rotational correlation time (τ_R) of $[\text{Gd}(\text{TTDA-MA})(\text{H}_2\text{O})]^-$, $[\text{Gd}(\text{TTDA-BA})(\text{H}_2\text{O})]^-$, and $[\text{Gd}(\text{TTDA-MOBA})(\text{H}_2\text{O})]^-$ are obtained from reduced the ^{17}O relaxation rate and chemical shifts of H_2^{17}O . The ^2H NMR longitudinal relaxation rates of the deuterated diamagnetic lanthanum complexes for the rotational correlation time were also thoroughly investigated. The water-exchange rates (k_{ex}^{298}) for $[\text{Gd}(\text{TTDA-MA})(\text{H}_2\text{O})]^-$, $[\text{Gd}(\text{TTDA-BA})(\text{H}_2\text{O})]^-$, and $[\text{Gd}(\text{TTDA-MOBA})(\text{H}_2\text{O})]^-$ are lower than that of $[\text{Gd}(\text{TTDA})(\text{H}_2\text{O})]^{2-}$ but significantly higher than those of $[\text{Gd}(\text{DTPA})(\text{H}_2\text{O})]^{2-}$ and $[\text{Gd}(\text{DTPA-BMA})(\text{H}_2\text{O})]$. The rotational correlation times for $[\text{Gd}(\text{TTDA-BA})(\text{H}_2\text{O})]^-$ and $[\text{Gd}(\text{TTDA-MOBA})(\text{H}_2\text{O})]^-$ are significantly longer than those of $[\text{Gd}(\text{TTDA})(\text{H}_2\text{O})]^{2-}$ and $[\text{Gd}(\text{DTPA})(\text{H}_2\text{O})]^{2-}$ complexes. The marked increase of the relaxivity of $[\text{Gd}(\text{TTDA-BA})(\text{H}_2\text{O})]^-$ and $[\text{Gd}(\text{TTDA-MOBA})(\text{H}_2\text{O})]^-$ results mainly from their longer rotational correlation time. The noncovalent interaction between human serum albumin (HSA) and $[\text{Gd}(\text{TTDA-BA})(\text{H}_2\text{O})]^-$ and $[\text{Gd}(\text{TTDA-MOBA})(\text{H}_2\text{O})]^-$ complexes containing a hydrophobic substituent was investigated by measuring the water proton relaxation rate of the aqueous solutions. The binding association constant (K_A) values are $1.0 \pm 0.2 \times 10^3$ and $1.3 \pm 0.2 \times 10^3 \text{ M}^{-1}$ for $[\text{Gd}(\text{TTDA-BA})(\text{H}_2\text{O})]^-$ and $[\text{Gd}(\text{TTDA-MOBA})(\text{H}_2\text{O})]^-$, which indicates a stronger interaction of $[\text{Gd}(\text{TTDA-BA})(\text{H}_2\text{O})]^-$ and $[\text{Gd}(\text{TTDA-MOBA})(\text{H}_2\text{O})]^-$ with HSA.

Introduction

The search for macromolecular Gd(III) complexes to be used in magnetic resonance imaging (MRI) has gone on over the past two decades.^{1–3} These macromolecular systems

provide both an enhanced ability to catalyze solvent proton relaxation through a long molecular reorientation time and an increased lifetime of the contrast agents in the circulating blood by avoiding the extravasation of the contrast agents of the small molecular Gd(III) complexes commonly employed in MRI investigations.⁴ The water-residence lifetime has little influence on relaxivity for small molecular contrast agents, but it shows significant influence on macromolecular contrast agents. Hence, $[\text{Gd}(\text{TTDA})]^{2-}$ (TTDA = EPTPA

* To whom correspondence should be addressed. E-mail: ymwang@kmu.edu.tw. Phone: 886-7-3121101 ext 2218. Fax: 886-7-3125339.

[†] Faculty of Medicinal and Applied Chemistry.

[‡] Graduate Institute of Pharmaceutical Sciences.

[§] Department of Medical Imaging.

- (1) Spanoghe, M.; Lanens, D.; Dommissie, R.; Van Der Linden, A.; Alderweireldt, F. *Magn. Reson. Imaging* **1992**, *10*, 913.
- (2) Aime, S.; Botta, M.; Crich, S. G.; Giovenzana, G.; Palmisano, G.; Sisti, M. *Bioconjugate Chem.* **1999**, *10*, 192.

- (3) Doble Dan, M. J.; Botta, M.; Wang, J.; Aime, S.; Barge, A.; Raymond, K. N. *J. Am. Chem. Soc.* **2001**, *123*, 10758.

- (4) Lauffer, R. B. *Chem. Rev.* **1987**, *87*, 901.

stand at room temperature overnight. The crystalline product TTDA-4est was isolated by filtration, washed with ethyl acetate, and dried in a vacuum. The product was recrystallized from ethyl acetate, yielding 47.5 g (46.9%): mp 105.1–106.4 °C. Anal. Calcd for $C_{29}H_{55}N_3O_8$ (fw = 573.77): C, 60.71; H, 9.66; N, 7.32. Found: C, 60.59; H, 9.75; N, 7.21. 1H NMR ($CDCl_3$, 400 MHz), δ (ppm): 3.56 (s, 4H, $-CH_2COOtBu$), 3.51 (s, 4H, $-CH_2COOtBu$), 3.27 (t, $J = 14$ Hz, 2H, ethylene backbone), 3.22 (t, $J = 14$ Hz, 2H, propylene backbone), 3.06 (t, $J = 14$ Hz, 2H, ethylene backbone), 2.90 (t, $J = 14$ Hz, 2H, propylene backbone), 2.07 (m, 2H, $-NCH_2CH_2CH_2N-$), 1.45 (s, 36H, $-C(CH_3)_3$). ^{13}C NMR ($CDCl_3$, 400 MHz), δ (ppm): 171.1, 170.8, 81.6, 81.3, 55.2, 54.9, 52.1, 50.3, 49.2, 45.9, 28.1, 22.9.

6-(Methoxycarbonylmethyl)-3,10-di(carboxymethyl)-3,6,10-triazadodecanedioic, (Tetra)-tert-butyl Ester (TTDA-4est-OMe, 3). Tetramethylguanidine (TMG)(10.3 mL, 87.2 mmol) was added to a stirred solution of TTDA-4est (5.0 g, 8.7 mmol) in CH_3CN (50 mL), and the mixture was stirred for 30 min at 10 °C. Methyl bromoacetate (1.1 mL, 11.3 mmol) was added in one portion, and the resulting mixture was stirred and refluxed overnight and then evaporated in a vacuum. To the residue was added distilled water to dissolve tetramethylguanidine. The hydrate was removed by filtering the reaction mixture with a Büchner funnel and washing with distilled water. The oil phase was dissolved by acetone and evaporated under reduced pressure. The product was purified by column chromatography (SiO_2 , ethyl acetate/hexane 2:3), yielding 3.4 g (60.1%) of TTDA-4est-OMe as a colorless viscous oil. Anal. Calcd for $C_{32}H_{59}N_3O_{10}$ (fw = 645.83): C, 59.51; H, 9.21; N, 6.51. Found: C, 59.44; H, 9.32; N, 6.63. 1H NMR ($CDCl_3$, 400 MHz), δ (ppm): 3.67 (s, 3H, $COOCH_3$), 3.44 (s, 4H, $-CH_2COOtBu$), 3.41 (s, 4H, $-CH_2COOtBu$), 2.84 (t, 2H, $J = 7.2$ MHz, $-CH_2-$), 2.75 (t, $J = 7.2$ MHz, 2H, $-CH_2-$), 2.69 (t, $J = 7.2$ MHz, 2H, $-CH_2-$), 2.64 (t, $J = 7.2$ MHz, 2H, $-CH_2-$), 1.63 (p, $J = 7.2$ MHz, 2H, $-NCH_2CH_2CH_2N-$), 1.45 (s, 36H, $-C(CH_3)_3$). ^{13}C NMR ($CDCl_3$, 400 MHz), δ (ppm): 172.01, 170.66, 80.83, 80.79, 56.14, 55.77, 54.75, 52.63, 52.53, 52.24, 52.06, 51.23, 28.15, 26.16.

General Procedure for the Reaction of TTDA-4est-OMe (3) with Methylamine, Benzylamine, or 2-Methoxybenzylamine. To a stirred solution of TTDA-4est-OMe (4.0 g, 6.2 mmol) was added methylamine (2.1 mL, 61.9 mmol), benzylamine (6.8 mL, 61.9 mmol), or 2-methoxybenzylamine (8.1 mL, 61.9 mmol), after which the mixture was stirred and refluxed overnight and then evaporated in a vacuum. Then, 2 N HCl (50 mL) was added to the residue, and the mixture was stirred for 12 h at room temperature. The salt was removed by filtering the reaction mixture with a Büchner funnel, and it was washed with distilled water. The filtrate was evaporated by rotary evaporation. Then, the oil was obtained and dissolved in 20 mL of distilled water, alkalized with ammonia water to pH 11.0, and the solution applied to an AG1 \times 8 anion-exchange resin column (200–400 mesh, HCO_2^- form, 100 mL of resin, 3.0 cm column diameter). The product was eluted with 500 mL of water and a formic acid gradient.

6-[(Methylcarbamoyl)methyl]-3,6,10-tri(carboxymethyl)-3,6,10-triazadodecanedioic Acid (TTDA-MA, 4). The product TTDA-MA came off in 0.6 N formic acid, yielding 1.2 g (46.2%). MS (ESI): m/z : 420.19 $[M + H]^+$. Anal. Calcd for $C_{16}H_{28}N_4O_9$ (fw = 420.42): C, 45.71; H, 6.71; N, 13.33. Found: C, 45.83; H, 6.62; N, 13.42. 1H NMR (D_2O , 400 MHz), δ (ppm): 3.86 (s, 4H, $-CH_2COOH$), 3.70 (s, 4H, $-CH_2COOH$), 3.81 (s, 2H, $-CH_2CONCH_3$), 3.31 (t, $J = 8.0$ MHz, 2H, $-CH_2-$), 3.29 (t, $J = 8.0$ MHz, 2H, $-CH_2-$), 3.27 (t, $J = 8.0$ MHz, 2H, $-CH_2-$), 3.14 (t, $J = 7.6$ MHz, 2H, $-CH_2-$), 2.71 (s, 3H, $-CONCH_3$), 2.06 (p, $J = 3.2$ MHz, 2H, $-NCH_2CH_2CH_2N-$). ^{13}C NMR (D_2O , 400 MHz),

δ (ppm): 172.77, 169.67, 167.84, 56.70, 56.00, 54.97, 53.41, 52.27, 51.96, 50.48, 25.85, 19.84.

6-[(Benzylcarbamoyl)methyl]-3,6,10-tri(carboxymethyl)-3,6,10-triazadodecanedioic Acid (TTDA-BA, 5). The product TTDA-BA came off in 1.1 and 1.2 N formic acid, yielding 1.7 g (54.7%). MS (ESI): m/z : 496.22 $[M + H]^+$. Anal. Calcd for $C_{22}H_{32}N_4O_9$ (fw = 496.51): C, 53.22; H, 6.50; N, 11.28. Found: C, 53.13; H, 6.38; N, 11.13. 1H NMR (D_2O , 400 MHz), δ (ppm): 7.36–7.27 (m, $J = 7.6$ MHz, 5H, $-C_6H_5$), 4.367 (s, 2H, $-CONCH_2C_6H_5$), 3.95 (s, 2H, $-CH_2CONCH_2C_6H_5$), 3.84 (s, 4H, $-CH_2COOH$), 3.61 (s, 4H, $-CH_2COOH$), 3.28–3.203 (m, $J = 8.0$ MHz, 8H, $-CH_2-$), 2.05 (p, $J = 3.2$ MHz, 2H, $-N-CH_2CH_2CH_2N-$). ^{13}C NMR (D_2O , 400 MHz), δ (ppm): 172.43, 169.16, 166.68, 137.15, 128.51, 127.33, 127.16, 56.251, 55.57, 54.69, 52.98, 52.25, 51.97, 50.10, 42.92, 19.51.

6-[(2-Methoxybenzylcarbamoyl)-methyl]-3,6,10-tri(carboxymethyl)-3,6,10-triazadodecanedioic Acid (TTDA-MOBA, 6). The product TTDA-MOBA came off in 0.9 N formic acid, yielding 1.7 g (52.5%). MS (ESI): m/z : 526.23 $[M + H]^+$. Anal. Calcd for $C_{22}H_{32}N_4O_9$ (fw = 526.54): C, 52.46; H, 6.51; N, 10.64. Found: C, 52.35; H, 6.58; N, 10.72. 1H NMR(D_2O , 400 MHz), δ (ppm): 7.25–6.90 (m, $J = 22.4$ MHz, $J = 17.6$ MHz, 4H, $-C_6H_4OCH_3$), 4.30 (s, 2H, $-CONCH_2C_6H_4OCH_3$), 3.83 (s, 3H, $-OCH_3$), 3.75–3.57 (s, 2H, $-NCH_2CON-$, s, 8H, $-CH_2COOH$), 3.22–3.12 (m, $J = 7.6$ MHz, 8H, $-CH_2-$), 2.00 (p, $J = 3.2$ MHz, 2H, $-NCH_2CH_2CH_2N-$). ^{13}C NMR (D_2O , 400 MHz), δ (ppm): 172.82, 169.55, 166.61, 129.54, 129.41, 125.08, 120.79, 111.38, 56.58, 55.91, 55.53, 54.90, 53.23, 52.20, 50.35, 39.05, 19.75.

Complexation. The Gd(III), Dy(III), and La(III) complexes were prepared by dissolving the ligand (0.05 mmol) in H_2O (3 mL) and adjusting the pH of the solution to 7.5 with 1 N NaOH. To these solutions was added 2.5 mL of an aqueous solution of $LnCl_3$ (0.05 mmol) dropwise, maintaining the pH at 7.5 with 1 N NaOH. The Ln(III) chelate formations were instantaneous at room temperature. The free lanthanide ions in the solutions were confirmed by the xylenol orange test. The solutions were then evaporated under reduced pressure.

Potentiometric Measurements. The protonation constants of the ligands were determined by potentiometric titrations of 1.0 mM ligand solutions using an automatic titrator system. Stability constants of the Gd^{3+} , Ca^{2+} , Zn^{2+} , and Cu^{2+} complexes of ligands were also determined by direct titration of equimolar amounts of metal and ligand (1.0 mM). The autotitrating system consists of a 702 SM Titroprocessor, a 728 stirrer, and a PT-100 combination pH electrode (Metrohm). The protonation constants of the ligands were calculated using a FORTRAN computer program, PKAS,⁸ written for polyprotonic weak acid equilibria. The overall stability constants of the various metal complexes formed in aqueous solution were determined from the titration data with the FORTRAN computer program BEST.⁸

NMR pH Titration. Solutions of TTDA-MA (0.1 mM) for NMR pH titration were made up in D_2O , and the pD was adjusted with DCl or CO_2 -free NaOD. Proton NMR spectra were measured in D_2O solution on a Varian Gemini 400 spectrometer. The final pD values of the amide solutions were determined with a microelectrode. The final pD was obtained from the equation $pD = pH + 0.40$.⁹ The hydrogen electrode used in the present study allows a reliable and accurate determination of the proton activity over an

(8) Martell, A. E.; Motekaitis, R. J. *Determination and Use of Stability Constants*, 2nd ed.; VCH: New York, 1992.

(9) Aime, S.; Botta, M.; Frullano, L.; Crich, S. G.; Giovenzana, G.; Pagliarini, R.; Palmisano, G.; Sirtori, F. R.; Sisti, M. *J. Med. Chem.* **2000**, *43*, 4017.

Table 1. Protonation Constants of TTDA-MA, TTDA-BA, TTDA-MOBA, TTDA, EPTPA-bz-NO₂, and DTPA at $I = 0.1$ M Me₄NCl^a

equilibrium	log K_n					
	TTDA-MA	TTDA-BA	TTDA-MOBA	TTDA	EPTPA-bz-NO ₂ ^b	DTPA ^c
[HL]/[L][H]	10.22(0.03)	10.27(0.03)	10.61(0.03)	10.60	10.86	10.49
[H ₂ L]/[HL][H]	9.22(0.02)	8.90(0.02)	9.04(0.01)	8.9	8.91	8.60
[H ₃ L]/[H ₂ L][H]	3.29(0.02)	3.15(0.02)	3.02(0.03)	5.19	4.70	4.28
[H ₄ L]/[H ₃ L][H]	2.74(0.01)	2.85(0.01)	2.17(0.01)	2.95	3.25	2.64
[H ₄ L]/[H ₄ L][H]					2.51	
ΣpK_a	25.47	25.17	24.84	27.64	30.23	26.01

^a $T = 25.0 \pm 0.1$ °C. ^b Reference 6. ^c Reference 12.

extended pH range. All chemical shifts were referenced to the 3-(trimethylsilyl)-1-propanesulfonic acid.

Solution NMR. The ¹H NMR experiments were performed on a Varian Gemini 400 spectrometer with the probe air temperature regulated at 25 °C. Similar NMR studies on [La(TTDA-MA)]⁻ in solution have been described previously.⁷

Relaxation Time Measurement. The Gd(III) chelate solutions under various pH values were prepared by combining the buffer solution with an approximately diluted Gd(III) complex solution in a 1:1 (v/v) ratio.⁷ Relaxation times T_1 's of aqueous solutions of gadolinium(III) complexes of ligands were measured to determine relaxivity r_1 . All measurements were made using an NMR spectrometer operating at 20 MHz and 37.0 ± 0.1 °C (NMS 120 Minispec, Bruker), by means of the standard inversion–recovery pulse sequence.

Deuteration of Ligands. Deuteration of ligands at the α -position with respect to carbonyl groups was performed as follows: 2 mmol of ligand was dissolved in 20 mL of D₂O, the pD value was adjusted to 10.3 by addition of K₂CO₃, and the mixture was refluxed under stirring for 24 h. The pD was then adjusted to 2 with concentrated DCl solution, the solution concentrated to 5 mL and the solid KCl filtered off. Acetone was added to induce precipitation of the deuterated compound, which was then recovered by filtration and dissolved in D₂O. The solution was neutralized with NaOD, and the product was isolated after lyophilization.

²H NMR Measurements. The rotational correlation time values of [La(TTDA-MA)]⁻, [La(TTDA-BA)]⁻, and [La(TTDA-MOBA)]⁻ were determined by ²H NMR. The measurement was carried out in 10-mm (o.d.) tubes on a Varian Gemini-400 spectrometer equipped with a broadband probe. No field frequency lock was used.

¹⁷O NMR Measurement. The hydration number of [Dy(TTDA-MA)]⁻ was determined by the method of Alpoim et al.¹⁰ The ¹⁷O NMR spectra were recorded by a Varian Gemini 400 spectrometer at 25 °C. The dysprosium (Dy) induced ¹⁷O shift (d.i.s.) measurements were determined using D₂O as an external standard.

The measurement of the ¹⁷O transverse relaxation rates, longitudinal relaxation rates, and chemical shifts was carried out with a Varian Gemini-400 spectrometer, equipped with a 10 mm probe, by using an external D₂O lock. The Varian 600 temperature control unit was used to stabilize the temperature in the range 5–75 °C. Solutions containing 5.5% of the ¹⁷O isotope were used. The inversion recovery of method was applied to measure longitudinal relaxation rates, $1/T_1$'s, and the Carr–Purcell–Meiboom–Gill spin–echo technique was used to obtain transverse relaxation rates, $1/T_2$'s. The solution was introduced into spherical glass containers, fitting into ordinary 10-mm NMR tubes, in order to eliminate magnetic susceptibility corrections to chemical shifts.

Data Analysis. The simultaneous least-squares fitting of ¹⁷O NMR data and the binding parameters to HSA were determined by fitting the experimental data using the program *SCIENTIST* for WINDOWS by *MICROMATH*, version 2.0.

Results and Discussion

Synthesis of the Ligands. TTDA-4est was synthesized from the commercially available *N*-(2-aminoethyl)-1,3-propanediamine and treated with *tert*-butylbromoacetate. The yield obtained by extraction of the crude compound with chloroform and then recrystallization from ethyl acetate is 46.9%, which is higher than that of material that was only recrystallized from ethyl acetate (25.5%). To a stirred solution of the TTDA-4est were added the tetramethylguanidine (TMG) and methyl bromoacetate, and the mixture was refluxed. The crude product was then purified by column chromatography, and it yielded a colorless viscous oil. Finally, the methylamine, benzylamine, and 2-methoxybenzylamine were added to a solution of TTDA-4est-OME, respectively. The mixture was stirred and refluxed overnight and then evaporated in a vacuum to obtain the final compounds TTDA-MA, TTDA-BA, and TTDA-MOBA.

Protonation Constants. The potentiometric titration curves for TTDA and TTDA-monoamide derivatives have been deposited as Supporting Information (Figures 1S–4S). Table 1 summarizes the protonation constants of TTDA-MA, TTDA-BA, TTDA-MOBA, TTDA,¹¹ and DTPA.¹² The titration curves of TTDA-MA, TTDA-BA, and TTDA-MOBA show a significant increase in the pH value at $a = 2$ ($a =$ moles of base per mol ligand present), respectively. This is due to the large difference between the second (log K_2) and third protonation constant (log K_3), i.e., 9.22 and 3.29; 8.90 and 3.15; 9.04 and 3.02, respectively. The first and second protonation constants of TTDA-MA, TTDA-BA, and TTDA-MOBA are similar to those of TTDA and EPTPA-bz-NO₂.⁶ The third protonation constants of TTDA-MA, TTDA-BA, and TTDA-MOBA are significantly lower than that of TTDA. The ΣpK_a values of TTDA-MA, TTDA-BA, and TTDA-MOBA are significantly lower than those of TTDA, EPTPA-bz-NO₂, and DTPA.

The macroscopic protonation constants of the TTDA-monoamide derivatives in Table 1 determined by the potentiometric titration technique do not give any indication of the specific preference of the protonation sites. However,

(10) Alpoim, M. C.; Urbano, A. M.; Galdes, C. F. G. C.; Peters, J. A. *J. Chem. Soc., Dalton Trans.* **1992**, 463.

(11) Wang, Y. M.; Lee, C. H.; Liu, G. C.; Sheu, R. S. *J. Chem. Soc., Dalton Trans.* **1998**, 4113.

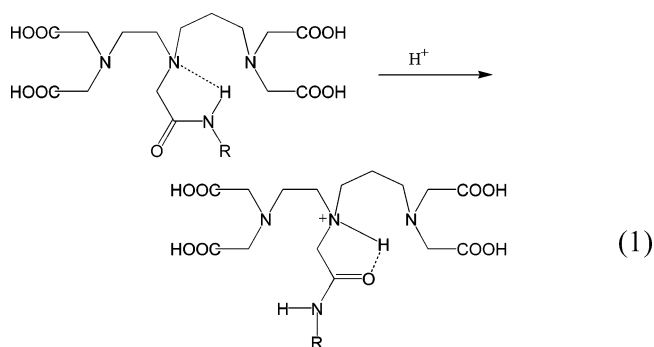
(12) Cachet, W. P.; Quay, S. C.; Rocklage, S. M. *Magn. Reson. Imaging* **1990**, 8, 467.

Table 2. Stability Constants, Conditional Stability Constants, Selectivity Constants and Modified Selectivity Constants of Gd^{3+} , Zn^{2+} , Ca^{2+} , and Cu^{2+} Complexes with TTDA-MA, TTDA-BA, TTDA-MOBA, TTDA, EPTPA-bz-NO₂, and DTPA, at $I = 0.10$ N (CH₃)₄NCl and 25.0 ± 0.1 °C^a

parameter	log K_{ML}					
	TTDA-MA	TTDA-BA	TTDA-MOBA	TTDA	EPTPA-bz-NO ₂ ^b	DTPA ^c
[GdL]/[Gd][L]	16.71(3)	16.94(2)	16.93(2)	18.96 (18.75) ^b	19.20	22.46
log K_{GdL} (pH 7.4)	12.06	12.56	12.07	14.25		18.14
[CaL]/[Ca][L]	10.81(2)	10.87(4)	10.49(5)	9.13(1)	9.38	10.75
log K_{CaHL}	8.53(2)	8.90(1)	8.18(7)	8.20(1)		6.11
log K_{CaL} (pH 7.4)	6.16	6.49	5.63	4.42		6.43
[ZnL]/[Zn][L]	13.10(2)	13.04(5)	13.14(2)	16.03(2)	16.01	18.70
log K_{ZnHL}	7.73(4)	7.52(4)	7.59(7)	7.80(3)		5.60
log K_{ZnL} (pH 7.4)	8.45	8.66	8.28	11.32		14.38
[CuL]/[Cu][L]	15.14(2)	14.91(4)	15.05(3)	16.77(6)	18.47	21.38
log K_{CuHL}	4.87(5)	5.36(4)	5.39(7)	5.69(5)		4.81
log K_{CuL} (pH 7.4)	10.49	10.53	10.19	12.06		17.0
selectivity [log $K(Gd/Zn)$]	3.61	3.90	3.79	2.93	3.19	3.76
selectivity [log $K(Gd/Ca)$]	5.90	6.07	6.44	9.83	9.82	11.71
selectivity [log $K(Gd/Cu)$]	1.57	2.03	1.88	2.19	0.73	1.08
log K_{sel} ^e	7.37	7.75	7.65	7.18		7.06

^a Uncertainty (σ) in log K values are given in parentheses. ^b Reference 6. ^c Reference 12.

the microscopic protonation scheme that is obtained by NMR spectroscopy coupled with pH titration does give this indication. This is constructed by measuring the chemical shifts of the methylenic protons as a function of pH. The deshielding of adjacent methylene protons is based on the protonation of a basic site of a poly(aminocarboxylate) in acidic solution. The proton NMR spectra of TTDA-MA as a function of pH and plots of the chemical shift values (δ) of the methylenic resonance of TTDA-MA as a function of pH have been deposited as Supporting Information (Figures 5S–6S). The downfield shift of δ in the region pH 11.0–9.0 indicates that the first and second observed protonations occurred on the terminal propylene nitrogen and ethylene nitrogen atoms, respectively. The third protonation occurred on the central nitrogen atom. Therefore, the third protonation constant of TTDA-monoamide is significantly lower than that of TTDA because of the formation of a hydrogen bond between the central nitrogen atom and the amide NH proton shown in eq 1, which reduces the basicity of the central nitrogen atom.



Thermodynamic Stability Constants. The metal chelates thermodynamic stability constants (K_{ML} 's) are expressed as in eq 2

$$K_{ML} = [ML]/[M][L] \quad (2)$$

where M represents the free, unhydrolyzed aquametal ion, L is the uncomplexed, totally deprotonated form of the ligand, and ML is the normal unprotonated and unhydrolyzed

complex. The potentiometric titration curves for the complexes of Gd^{3+} , Ca^{2+} , Cu^{2+} , and Zn^{2+} with TTDA-monoamide derivatives have been deposited as Supporting Information (Figures 1S–3S). In addition, the thermodynamic stability constants of TTDA chelates have been redetermined and deposited as Supporting Information (Figure 4S) since Merbach et al.⁶ questioned the stability constant values of TTDA (TTDA = EPTPA) complexes with Gd^{3+} and Ca^{2+} that we had previously published.⁵ The stability constant value of $[Gd(TTDA)]^{2-}$ in this study is similar to that of the previously results of Merbach et al.⁶ shown in Table 2 (in parentheses). Also, the stability constant $[Ca(TTDA)]^{3-}$ is similar to that of $[Ca(EPTPA-bz-NO_2)]^{3-}$. The thermodynamic stability constants of metal chelates with TTDA-MA, TTDA-BA, TTDA-MOBA, TTDA, EPTPA-bz-NO₂,⁶ and DTPA¹² are shown in Table 2. The stability constants of $[Gd(TTDA-MA)]^{-}$, $[Gd(TTDA-BA)]^{-}$, and $[Gd(TTDA-MOBA)]^{-}$ are significantly lower than those of $[Gd(TTDA)]^{2-}$, $[Gd(EPTPA-bz-NO_2)]^{2-}$, and $[Gd(DTPA)]^{2-}$. The lower stability constants of the TTDA-monoamide derivatives chelates with Gd^{3+} , Ca^{2+} , Zn^{2+} , and Cu^{2+} when compared to those of TTDA, EPTPA-bz-NO₂, and DTPA chelates may be ascribed to the low basicity of TTDA-monoamide derivatives. In Table 2, the order of conditional stability constant at pH 7.4 is $[Gd(DTPA)]^{2-} > [Gd(TTDA)]^{2-} > [Gd(TTDA-monoamide)]^{-}$.

Selectivity Constants and Modified Selectivity Constants. The logarithmic selectivity constant¹³ of TTDA-MA, TTDA-BA, TTDA-MOBA, TTDA, EPTPA-bz-NO₂, and DTPA for Gd^{3+} over Ca^{2+} , Zn^{2+} , and Cu^{2+} is the difference between log K_{GdL} and log K_{ML} ($M = Ca^{2+}$, Zn^{2+} , or Cu^{2+}); i.e., log $K(Gd - Ca)$, log $K(Gd - Zn)$, and log $K(Gd - Cu)$ are also listed in Table 2. From the selectivity constants, the log $K(Gd - Zn)$ values of TTDA-monoamide derivatives are similar to that of DTPA. However, the selectivity constant value (log $K(Gd - Zn)$) of TTDA-monoamide derivatives is higher than those of TTDA and EPTPA-bz-NO₂. In other words, the TTDA-monoamide derivatives show similar

(13) Kumar, K.; Tweedle, M. F.; Malley, M. F.; Gougoutas, J. Z. *Inorg. Chem.* **1995**, *34*, 6472.

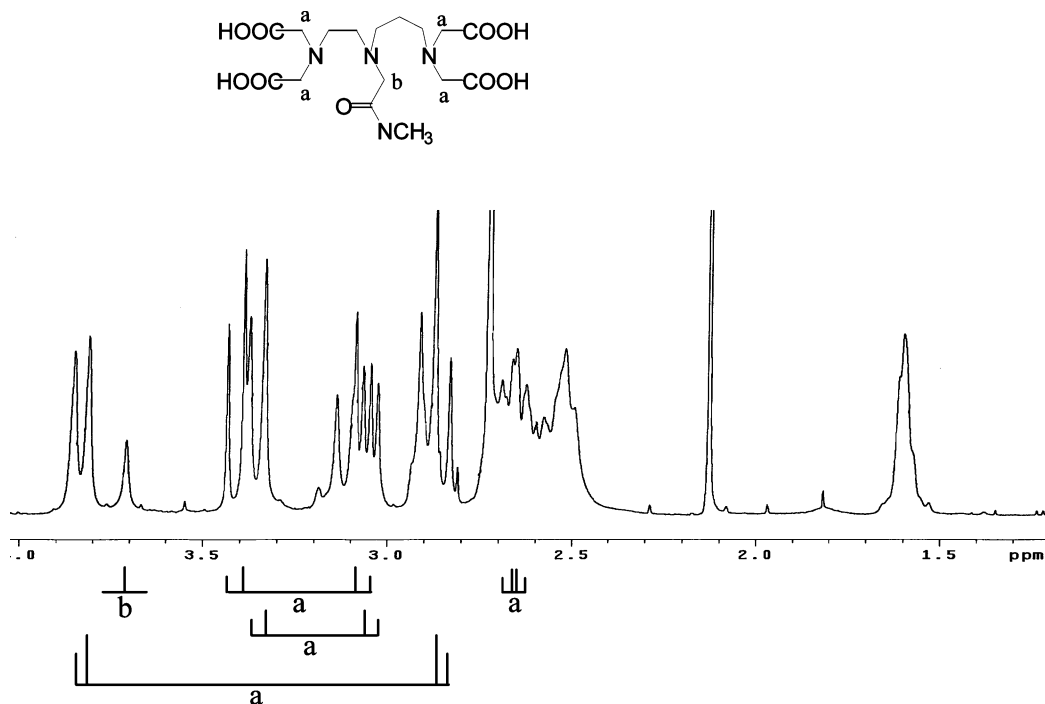


Figure 1. ^1H NMR spectrum of $[\text{La}(\text{TTDA-MA})]^-$ at 25 °C.

favorable selectivity toward Gd^{3+} over Zn^{2+} . The modified selectivity constant (K_{sel}) value for Gd^{3+} over other endogenous metal ions (Ca^{2+} , Zn^{2+} , and Cu^{2+}) and H^+ for a ligand can be calculated and is obtained by the incorporation of ligand equilibria with Ca^{2+} , Zn^{2+} , Cu^{2+} , and H^+ .¹² Table 2 shows the modified selectivity constants of TTDA-MA, TTDA-BA, TTDA-MOBA, TTDA, and DTPA at pH 7.4. The concentrations of Ca^{2+} , Zn^{2+} , and Cu^{2+} used here were 2.5, 5.0×10^{-2} , and 1.0×10^{-3} mM, respectively.¹² The $\log K_{\text{sel}}$ values of TTDA-MA (7.37), TTDA-BA (7.75), and TTDA-MOBA (7.65) are higher than those of TTDA (7.18) and DTPA (7.06). Thus, TTDA-monoamide derivatives form Gd^{3+} complexes that are slightly more stable than that of $[\text{Gd}(\text{TTDA})]^{2-}$ toward transmetalation with Ca^{2+} , Zn^{2+} , and Cu^{2+} metal ions at pH 7.4.

Solution NMR of La(III) Chelate. The solution ^1H NMR spectrum of 30 mM $[\text{La}(\text{TTDA-MA})]^-$ in D_2O at pD 7.0 and 25 °C is shown in Figure 1. The peak assignments were also confirmed by 2D COSY spectrum at the same time and are deposited as Supporting Information (Figure 7S). The protons of the terminal acetate groups (H_a) give four AB patterns with the baricenter at 3.32 ppm ($J = 40$ Hz), 3.24 ppm ($J = 41$ Hz), 3.19 ppm ($J = 41$ Hz), and 2.65 ppm ($J = 40$ Hz), respectively. The lack of the fifth AB pattern indicates that there are only four carboxylate groups bound to La(III) ion and that the fifth amide oxygen atom is not bound to La(III) ion. This result is similar to the solution NMR study of $[\text{La}(\text{DTPA})]^{2-}$,^{14,15} and $[\text{La}(4(\text{S})\text{-bz-TTDA})]^{2-}$.⁷ In the case of $[\text{La}(\text{DTPA})]^{2-}$, there are two different AB patterns for the four terminal acetate groups and a singlet for the middle acetate, which indicates that the central carboxylate is not coordinated in the La(III) complex.

Dy(III)-Induced ^{17}O Water NMR shifts. The Dy(III)-induced water ^{17}O NMR shifts against Dy(III) chelate

concentration for solution of DyCl_3 and $[\text{Dy}(\text{TTDA-MA})(\text{H}_2\text{O})]^-$ in D_2O at 25 °C are deposited as Supporting Information (Figure 8S). The slopes obtained at pH = 5.0 is -45.5 ppm/mM ($r^2 = 0.998$) for $[\text{Dy}(\text{TTDA-MA})(\text{H}_2\text{O})]^-$. The slope for DyCl_3 is -384.9 ppm/mM ($r^2 = 0.999$), and a hydration number of eight has previously been proposed for the dysprosium(III) ion.^{16–18} Therefore, the $[\text{Dy}(\text{TTDA-MA})(\text{H}_2\text{O})]^-$ complex at pH 5.0 contains 0.9 inner-sphere water molecules per Dy(III) ion. The number of inner-sphere water molecules for $[\text{Dy}(\text{TTDA-BA})(\text{H}_2\text{O})]^-$ and $[\text{Dy}(\text{TTDA-MOBA})(\text{H}_2\text{O})]^-$ may be similar to that of $[\text{Dy}(\text{TTDA-MA})(\text{H}_2\text{O})]^-$. The number of Ln(III)-bound water molecules in complexes provides information for the coordination mode of the ligand. The coordination sites of Gd(III) ion for Gd^{3+} complexes with TTDA-monoamide derivatives are occupied by one water molecule, while eight sites are available for three amine nitrogen atoms, four carboxylate oxygen atoms, and one amide oxygen atom in the TTDA-monoamide ligand molecules.

Relaxometric Studies of the Gd(III) Complex. The paramagnetic contribution of the solvent longitudinal relaxation is obtained by the following eq 3¹⁹

$$R_{1p}^{\text{is}} = Cq/[55.6(T_{1M} + \tau_M)] \quad (3)$$

where C is the molar concentration of the gadolinium(III) complex, q is the number of water molecules bound to metal

- (14) Choppin, G. R.; Baisden, P. A.; Khan, S. A. *Inorg. Chem.* **1979**, *18*, 1330.
- (15) Peters, J. A. *Inorg. Chem.* **1988**, *27*, 4686.
- (16) Kowall, T.; Foglia, F.; Helm, L.; Merbach, A. E. *J. Am. Chem. Soc.* **1995**, *117*, 3790.
- (17) Cossy, C.; Helm, L.; Powell, D. H.; Merbach, A. E. *New J. Chem.* **1995**, *19*, 27.
- (18) Cossy, C.; Barnes, A. C.; Enderby, J. E.; Merbach, A. E. *J. Chem. Phys.* **1989**, *90*, 3254.

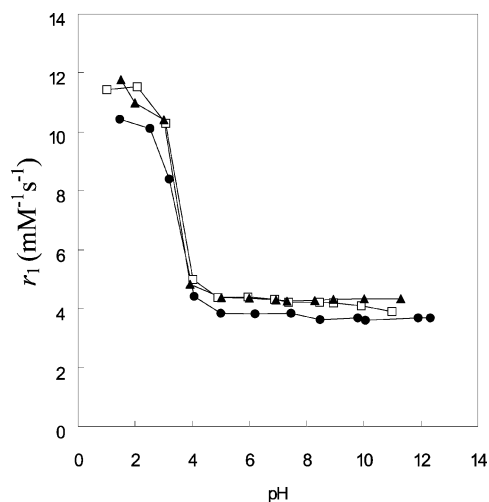


Figure 2. pH dependence of the relaxivity for $[\text{Gd}(\text{TTDA-MA})(\text{H}_2\text{O})]^-$ (●), $[\text{Gd}(\text{TTDA-BA})(\text{H}_2\text{O})]^-$ (□), and $[\text{Gd}(\text{TTDA-MOBA})(\text{H}_2\text{O})]^-$ (▲) at 37 °C and 20 MHz.

ions, T_{1M} is the longitudinal relaxation time of the bound water protons, and τ_M is the residence lifetime of the bound water. Because of the opposite temperature dependence of T_{1M} and τ_M , two cases can be considered: (1) fast water-exchange ($T_{1M} \gg \tau_M$), R_{1p}^{is} increases follow a single-exponential law with the decreasing temperature; (2) slow water-exchange ($T_{1M} \ll \tau_M$), R_{1p}^{is} increases follow a nonexponential law with the decreasing the temperature.²⁰

The spin–lattice relaxivity (r_1) values of gadolinium(III) complexes with TTDA-monoamide derivatives have been deposited as Supporting Information (Table 1S). The relaxivity value of $[\text{Gd}(\text{TTDA-MA})]^-$ is similar to those of $[\text{Gd}(\text{DTPA})]^{2-}$,²¹ $[\text{Gd}(\text{TTDA})]^{2-}$,¹¹ and $[\text{Gd}(\text{DTPA-BMA})]$.²² However, the relaxivity values of $[\text{Gd}(\text{TTDA-BA})]^-$ and $[\text{Gd}(\text{TTDA-MOBA})]^-$ are significantly higher than those of $[\text{Gd}(\text{DTPA})]^{2-}$, $[\text{Gd}(\text{TTDA})]^{2-}$, and $[\text{Gd}(\text{DTPA-BMA})]$. The relaxivity values for gadolinium(III) complexes with TTDA-monoamide derivatives at various pH values are shown in Figure 2, and their relaxivity curves exhibit no pH dependence over the pH range 4.0–12.0. In other words, no free ligand or free Gd(III) ion dissociation for $[\text{Gd}(\text{TTDA-MA})]^-$, $[\text{Gd}(\text{TTDA-BA})]^-$, and $[\text{Gd}(\text{TTDA-MOBA})]^-$ complexes occurred in the pH range of the solution. It is also concluded that the hydration number of $[\text{Gd}(\text{TTDA-MA})]^-$, $[\text{Gd}(\text{TTDA-BA})]^-$, and $[\text{Gd}(\text{TTDA-MOBA})]^-$ complexes remains one coordinated water molecule over the pH range 4.0–12.0. The relaxivity of $[\text{Gd}(\text{TTDA-MA})]^-$, $[\text{Gd}(\text{TTDA-BA})]^-$, and $[\text{Gd}(\text{TTDA-MOBA})]^-$ complexes increases with decreasing pH values over the pH range 4.0–1.5, which could be attributed to the partial dissociation of Gd(III) complexes at lower pH values.

Water-Exchange Lifetime Studies of Gd(III) Complex.

The ^{17}O NMR relaxation rates and angular frequencies of the Gd(III) complex solutions, $1/T_1$, $1/T_2$, and ω , and of the

acidified water reference, $1/T_{1A}$, $1/T_{2A}$, and ω_A , were measured at 9.4 T. Moreover, the reduced relaxation rates and chemical shift, $1/T_{1r}$, $1/T_{2r}$, and $\Delta\omega_r$, can also be calculated. The data are fitted simultaneously according to eqs 3–11,^{23–28} which have been deposited as Supporting Information. The results for $[\text{Gd}(\text{TTDA-MA})(\text{H}_2\text{O})]^-$, $[\text{Gd}(\text{TTDA-BA})(\text{H}_2\text{O})]^-$, $[\text{Gd}(\text{TTDA-MOBA})(\text{H}_2\text{O})]^-$, and $[\text{Gd}(\text{TTDA})(\text{H}_2\text{O})]^{2-}$ are plotted in Figures 3 and 4 with the corresponding curve representing the result of the best fitting of the data according to equations.

As illustrated by Table 3, there are a large number of parameters influencing the data obtained by the different techniques. The ^{17}O NMR technique has the advantage that the outer-sphere contributions to the relaxation rates are negligibly small, which is because the oxygen nucleus is closer to the paramagnetic center when it is bound in the inner-sphere. In addition, the longitudinal relaxation rates are dominated by the dipole–dipole and quadrupolar relaxation rates. For these rates, at the fields employed, rotation determines the correlation time, while the transverse relaxation rates are dominated by scalar relaxation, which is insensitive to rotation of the Gd(III) complex. This scalar relaxation mechanism is highly efficient and often results in a kinetically controlled “slow-exchange” region at low temperatures. These factors allowed a better separation of certain parameters, especially those describing the water exchange process.

From Table 3, accurate estimations of k_{ex}^{298} values are 37.8×10^6 for $[\text{Gd}(\text{TTDA-MA})(\text{H}_2\text{O})]^-$, 29.6×10^6 for $[\text{Gd}(\text{TTDA-BA})(\text{H}_2\text{O})]^-$, 26.9×10^6 for $[\text{Gd}(\text{TTDA-MOBA})(\text{H}_2\text{O})]^-$, and $146 \times 10^6 \text{ s}^{-1}$ for $[\text{Gd}(\text{TTDA})(\text{H}_2\text{O})]^{2-}$. We can find that the k_{ex}^{298} values of $[\text{Gd}(\text{TTDA-MA})(\text{H}_2\text{O})]^-$, $[\text{Gd}(\text{TTDA-BA})(\text{H}_2\text{O})]^-$, and $[\text{Gd}(\text{TTDA-MOBA})(\text{H}_2\text{O})]^-$ are significantly higher than those of $[\text{Gd}(\text{DTPA})(\text{H}_2\text{O})]^{2-}$ ²⁴ and $[\text{Gd}(\text{DTPA-BMA})(\text{H}_2\text{O})]$ ²¹ but lower than those of $[\text{Gd}(\text{TTDA})(\text{H}_2\text{O})]^{2-}$ and $[\text{Gd}(\text{EPTPA-bz-NO}_2)(\text{H}_2\text{O})]^{2-}$.⁶ The kinetic and NMR parameters of $[\text{Gd}(\text{TTDA})(\text{H}_2\text{O})]^{2-}$ in this study are similar to previous results of Merbach et al. for $[\text{Gd}(\text{EPTPA})(\text{H}_2\text{O})]^{2-}$ and $[\text{Gd}(\text{EPTPA-bz-NO}_2)(\text{H}_2\text{O})]^{2-}$.⁶ The substitution of an acetate arm with an amide group on the linear poly(aminocarboxylate) ligand has been shown to cause a significant effect on the exchange lifetime.²⁹ The less negatively charged and less strongly coordinated group cannot be expected to pull the ligand more tightly around the metal center, thus decreasing the crowding at the water binding site and hence possibly giving rise to a shorter gadolinium–inner-sphere water oxygen distance and a lower water-exchange rate. Several examples show that when the

(19) Swift, T. J.; Connick, R. E. *J. Chem. Phys.* **1962**, *37*, 307.

(20) Aime, S.; Botta, M.; Fasano, M.; Terreno, E. *Acc. Chem. Res.* **1999**, *32*, 941.

(21) Weinmann, H. J.; Brasch, R. C.; Press, W. R.; Wesbey, G. E. *AJR, Am. J. Roentgenol.* **1984**, *142*, 619.

(22) Chang, C. A. *Invest. Radiol.* **1993**, *28*, 521.

(23) Reuben, J. *J. Phys. Chem.* **1971**, *75*, 3164.

(24) Powell, D. H.; Ni Dhubhghaill, O. M.; Pubanz, D.; Helm, L.; Lebedev, Y. S.; Schlaepfer, W.; Merbach, A. E. *J. Am. Chem. Soc.* **1996**, *118*, 9333.

(25) Toth, E.; Helm, L.; Merbach, A. E.; Hedinger, R.; Hegetschweiler, K.; Janossy, A. *Inorg. Chem.* **1998**, *37*, 4104.

(26) Brittain, H. G.; Desreux, F. F. *Inorg. Chem.* **1984**, *23*, 4459.

(27) Abragam, A. *The Principles of Nuclear Magnetism*; Oxford University Press: London, 1961.

(28) Micskei, K.; Helm, L.; Brucher, E.; Merbach, A. E. *Inorg. Chem.* **1993**, *32*, 3844.

(29) Ehnebohm, L.; Fjaertoft Pedersen, B. *Acta Chem. Scand.* **1992**, *46*, 126.

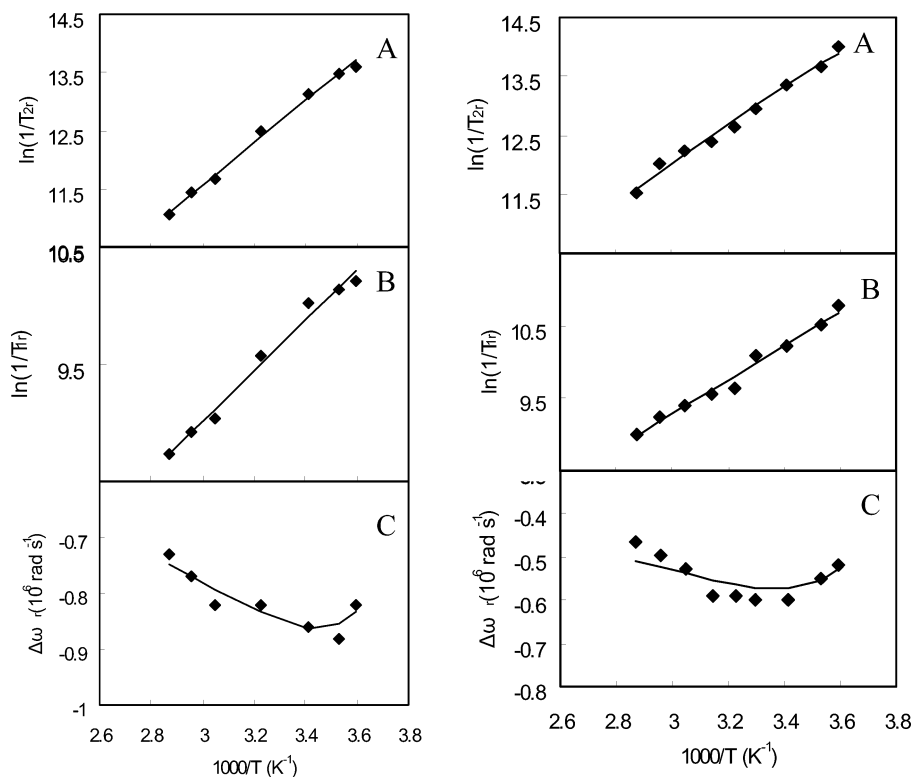


Figure 3. Temperature dependence of (A) transverse and (B) longitudinal ¹⁷O relaxation rates. (C) ¹⁷O chemical shifts at *B* = 9.4 T for [Gd(TTDA-MA)(H₂O)]⁻ (left) and [Gd(TTDA-BA)(H₂O)]⁻ (right). The lines represent simultaneous least-squares fits to all data points displayed.

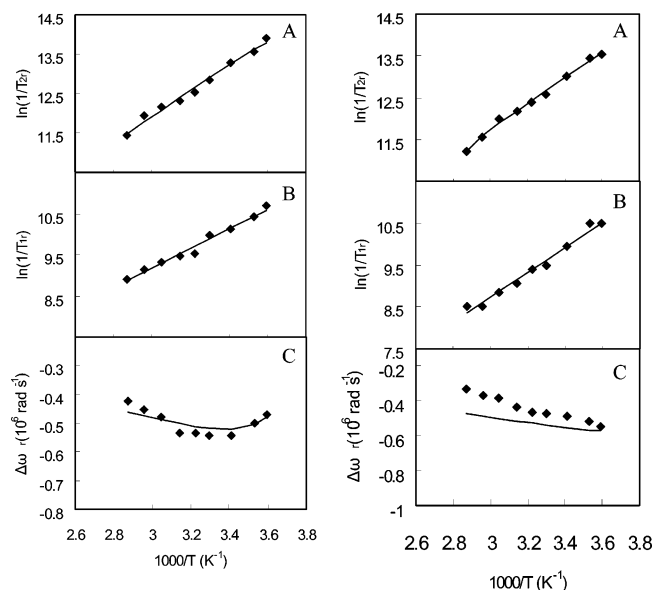


Figure 4. Temperature dependence of (A) transverse and (B) longitudinal ¹⁷O relaxation rates. (C) ¹⁷O chemical shifts at *B* = 9.4 T for [Gd(TTDA-MOBA)(H₂O)]⁻ (left) and [Gd(TTDA)(H₂O)]²⁻ (right). The lines represent simultaneous least-squares fits to all data points displayed.

negative charge is diminished by substituting a carboxylate group by the amide or hydroxyl, the water-exchange rate becomes slower.^{30–33} For example, for the gadolinium(III) complex of DTPA-bis(amide) derivatives, DTPA-BMA(1,7-

bis[*N*-methylcarbamoyl)methyl]-1,4,7-tris(carboxymethyl)-1,4,7-triazaheptane) and DTPA-BMEA (1,7-bis[*N*-methyl-ethylcarbamoyl)methyl]-1,4,7-tris(carboxymethyl)-1,4,7-triazaheptane), the water-exchange rate values are 0.45×10^6 and 0.39×10^6 s⁻¹, respectively,^{24,34} about one-eighth of the water-exchange rate on [Gd(DTPA)(H₂O)]²⁻. For the gadolinium(III) complex of each amide DOTA (1,4,7,10-tetraazacyclododecane-1,4,7,10-tetraacetate) derivative so far studied, the water-exchange rate is about one-fourth of k_{ex}^{298} on [Gd(DOTA)(H₂O)]⁻.²⁴ On the basis of all the k_{ex}^{298} values available for amide derivatives of either DTPA or DOTA, we can generally state that the replacement of one carboxylate group by an amide decreases the water-exchange rate of the gadolinium(III) complexes by a factor of about 4. On the basis of the water-exchange rate value available for [Gd(TTDA-MA)(H₂O)]⁻, [Gd(TTDA-BA)(H₂O)]⁻, and [Gd(TTDA-MOBA)(H₂O)]⁻, we can also generally state that the replacement of one carboxylate group by an amide group decreases the water-exchange rate of the gadolinium(III) complexes by a factor of about 5.

The activation volume (ΔV^\ddagger) for the water exchange reaction of [Gd(TTDA)(H₂O)]²⁻ has been determined (i.e., $\Delta V^\ddagger = +6.6$),⁶ and on the basis of the analogy to [Gd(TTDA)(H₂O)]²⁻, the water exchange has to be dissociatively activated for [Gd(TTDA-MA)(H₂O)]⁻, [Gd(TTDA-BA)(H₂O)]⁻, and [Gd(TTDA-MOBA)(H₂O)]⁻. The less negative activation entropies and the higher activation enthalpies of

- (30) Gonzalez, G.; Powell, D. H.; Tissieres, V.; Merbach, A. E. *J. Phys. Chem.* **1994**, *98*, 53.
 (31) Toth, E.; Vauthey, S.; Pubanz, D.; Merbach, A. E. *Inorg. Chem.* **1996**, *35*, 3375.
 (32) Toth, E.; Burai, L.; Brucher, E.; Merbach, A. E. *J. Chem. Soc., Dalton Trans.* **1997**, 1587.

- (33) Toth, E.; Pubanz, D.; Vauthey, S.; Helm, L.; Merbach, A. E. *Chem. Eur. J.* **1996**, *2*, 1607.
 (34) Toth, E.; Connac, F.; Helm, L.; Adzamlı, K.; Merbach, A. E. *Eur. J. Inorg. Chem.* **1998**, 2017.

Table 3. Kinetic and NMR Parameters of $[\text{Gd}(\text{TTDA-MA})(\text{H}_2\text{O})]^-$, $[\text{Gd}(\text{TTDA-BA})(\text{H}_2\text{O})]^-$, $[\text{Gd}(\text{TTDA-MOBA})(\text{H}_2\text{O})]^-$, $[\text{Gd}(\text{TTDA})(\text{H}_2\text{O})]^{2-}$, $[\text{Gd}(\text{TTDA-EPTPA-bz-NO}_2)(\text{H}_2\text{O})]^{2-}$, $[\text{Gd}(\text{DTPA-BMA})(\text{H}_2\text{O})]$, and $[\text{Gd}(\text{DTPA})(\text{H}_2\text{O})]^{2-}$ As Obtained from the Simultaneous Fit of ^{17}O NMR Data

parameter	TTDA-MA	TTDA-BA	TTDA-MOBA	TTDA	EPTPA ^a	EPTPA-bz-NO ₂ ^a	DTPA-BMA ^b	DTPA ^b
k_{ex}^{298} (10^6 s^{-1})	37.8 ± 2.4	29.6 ± 1.6	26.9 ± 2.0	146 ± 17	330 ± 40	150 ± 40	0.45 ± 0.01	3.3 ± 0.2
ΔH^\ddagger (kJ mol^{-1})	28.6 ± 0.9	29.3 ± 0.6	29.3 ± 0.8	23.1 ± 0.5	27.9 ± 1.1	-22.1 ± 1.8	47.6 ± 1.1	51.6 ± 1.4
ΔS^\ddagger ($\text{J mol}^{-1} \text{ K}^{-1}$)	-3.98 ± 2	-3.5 ± 1.8	-4.4 ± 1.6	-11.1 ± 3.1	11.0 ± 3.0	-9.1 ± 5.0	22.9 ± 3.6	53.0 ± 4.7
ΔV^\ddagger ($\text{cm}^3 \text{ mol}^{-1}$)					6.6 ± 0.3			
$A\hbar$ (10^6 rad s^{-1})	-3.9 ± 0.2	-2.7 ± 0.3	-2.4 ± 0.4	-3.2 ± 0.3	-3.9 ± 0.2	-3.2 ± 0.2	-3.8 ± 0.2	-3.8 ± 0.2
τ_{R}^{298} (ps)	103 ± 11 (80 ± 5)	132 ± 14 (108 ± 7)	145 ± 15 (130 ± 8)	104 ± 12	75 ± 6	122 ± 12	66 ± 11	58 ± 11
C_{os}	0	0	0	0			0.11 ± 0.04	0.18 ± 0.04
E_{R} (kJ mol^{-1})	17.9 ± 0.7	19.7 ± 0.8	19.6 ± 0.8	24.8 ± 1.5	17.7 ± 1.0	19.0 ± 1.7	21.9 ± 0.5	17.3 ± 0.8
method	^{17}O	^{17}O	^{17}O	^{17}O	^{17}O , EPR, NMRD	^{17}O , EPR, NMRD	^{17}O , EPR, NMRD	^{17}O , EPR, NMRD

^a Reference 6. ^b Reference 24.

$[\text{Gd}(\text{TTDA-MA})(\text{H}_2\text{O})]^-$, $[\text{Gd}(\text{TTDA-BA})(\text{H}_2\text{O})]^-$, and $[\text{Gd}(\text{TTDA-MOBA})(\text{H}_2\text{O})]^-$ seem to point to a more dissociative exchange as compared to $[\text{Gd}(\text{TTDA-bz-NO}_2)(\text{H}_2\text{O})]^{2-}$.⁶ Without the participation of the incoming water molecule, more energy is required to break the bond between the outgoing water molecule and the highly charged Gd^{3+} , leading to the higher ΔH^\ddagger values and lower k_{ex}^{298} values.

As has already been observed, the water-exchange rate decreases dramatically from $[\text{Gd}(\text{H}_2\text{O})_8]^{3+}$ to the chelate complexes with one inner-sphere water molecule, $[\text{Gd}(\text{TTDA})(\text{H}_2\text{O})]^{2-}$ and $[\text{Gd}(\text{DOTA})(\text{H}_2\text{O})]^{2-}$. This rate decrease is accompanied by an increase of ΔH^\ddagger . Since the results for $\text{Gd}(\text{III})$ complexes with TTDA-monoamide derivatives obey this trend, we thus conclude that water exchange on these complexes takes place most probably via a limiting dissociative D mechanism. The activation enthalpies for these three chelates are very similar. An amide group is coordinated less strongly toward the lanthanide ion than a carboxylate group, which is reflected by the lower stability constants of the amide complexes compared to carboxylate complexes in solution, and by the longer gadolinium–amide oxygen distance in the solid state, compared to carboxylate oxygen distances {e.g., the average gadolinium–carboxylate oxygen distance in $\text{Na}_2[\text{Gd}(\text{DTPA})(\text{H}_2\text{O})]$ is 0.240 nm,³⁵ and the amide oxygen distance in the DTPA-bis(benzylamide) complex of $\text{Gd}(\text{III})$ is 0.244 nm}.^{36,37} The consequence of the longer amide oxygen distance compared to carboxylate oxygen distance is a less crowded inner-sphere in the amide as compared to carboxylate complexes. A shorter gadolinium–inner-sphere water oxygen distance in the $\text{Gd}(\text{III})$ complexes with TTDA-monoamide derivatives was obtained compared to that of the $[\text{Gd}(\text{TTDA})(\text{H}_2\text{O})]^{2-}$ complex. Therefore, the activation enthalpy (ΔH^\ddagger) values for $\text{Gd}(\text{III})$ complexes with TTDA-monoamide derivatives are slightly higher than that of $[\text{Gd}(\text{TTDA})(\text{H}_2\text{O})]^{2-}$.

In addition to steric crowding, the reduced charge of the ligand may also play an important role. The trivalent gadolinium ion is not shielded as much by the coordination of an amide group as by a carboxylate. The remaining inner-

sphere water molecule will experience a stronger electrostatic attractive force from the metal center, which makes the dissociative step energetically disfavored compared to $[\text{Gd}(\text{TTDA})(\text{H}_2\text{O})]^{2-}$ complex.

For small $\text{Gd}(\text{III})$ chelates, the k_{ex}^{298} values of $[\text{Gd}(\text{TTDA-MA})(\text{H}_2\text{O})]^-$, $[\text{Gd}(\text{TTDA-BA})(\text{H}_2\text{O})]^-$, and $[\text{Gd}(\text{TTDA-MOBA})(\text{H}_2\text{O})]^-$ are significantly higher than that of $[\text{Gd}(\text{DTPA})(\text{H}_2\text{O})]^{2-}$,²⁴ but the relaxivity r_1 value of $[\text{Gd}(\text{TTDA-MA})(\text{H}_2\text{O})]^-$ ($3.89 \text{ mM}^{-1} \text{ s}^{-1}$) is very similar to those of $[\text{Gd}(\text{DTPA})(\text{H}_2\text{O})]^{2-}$,²⁰ $[\text{Gd}(\text{TTDA})(\text{H}_2\text{O})]^{2-}$, and $[\text{Gd}(\text{DTPA-BMA})(\text{H}_2\text{O})]^{2-}$ at 20 MHz and 37 ± 0.1 °C. It can be concluded that the mean residence lifetime (τ_{M}) does not contribute significantly to the relaxivity r_1 for the small molecule.³⁸

In diamagnetic molecules, the relaxation rate of the ^2H -nucleus is predominantly determined by a quadrupolar mechanism,^{39–42} which is strictly intramolecular and modulated solely by the rotation of the molecule. For fast-tumbling systems, the relaxation rate is thus directly related to the rotational correlation time shown in eq 4

$$R_1 = \frac{1}{T_1} = \frac{3}{8} \left(\frac{e^2 q Q}{h} \right)^2 \tau_{\text{R}} \quad (4)$$

where the quadrupolar coupling constant ($e^2 q Q/h$) depends on the hybridization state of the C-atom carrying the ^2H -atom, and its value is ca. 170 kHz in the case of an sp^3 C-atom. The measurement of τ_{R} was performed on the diamagnetic lanthanum(III) complex deuterated in the α -position relative to the carboxylate groups. At 298 K, the values of τ_{R} for $\text{La}(\text{III})$ complexes with TTDA-MA, TTDA-BA, and TTDA-MOBA are shown in Table 3 (in parentheses). The τ_{R} values of $[\text{La}(\text{TTDA-BA})(\text{H}_2\text{O})]^-$ and $[\text{La}(\text{TTDA-MOBA})(\text{H}_2\text{O})]^-$ are higher than that of $[\text{La}(\text{TTDA})(\text{H}_2\text{O})]^{2-}$. It is indicated that the replacement of the middle carboxylate group by a benzyl and methoxybenzyl amide group increases the τ_{R} value and causes the higher relaxivity of the Gd^{3+} complexes. The rotational dynamics of gadolinium(III)

(35) Cries, H.; Miklauta, H. *Physiol. Chem. Phys. Med. NMR* **1984**, *16*, 105.

(36) Wang, Y. M.; Cheng, T. H.; Sheu, R. S.; Chen, I. T.; Chiang, M. Y. *J. Chin. Chem. Soc.* **1997**, *44*, 123.

(37) Bligh, S. W. A.; Chowdhury, A. H. M. S.; McPartlin, M.; Scowen, I. J.; Bulman, R. A. *Polyhedron* **1995**, *14*, 567.

(38) Caravan, P.; Ellison, J. J.; McMurry, T. J.; Lauffer, R. B. *Chem. Rev.* **1999**, *99*, 2293.

(39) Mantsch, H. H.; Saito, H.; Smith, I. C. P. *Prog. Nucl. Magn. Reson. Spectrosc.* **1977**, *11*, 211.

(40) Van Haverbeke, Y.; Muller, R. N.; Vander Elst, L. *J. Phys. Chem.* **1984**, *88*, 4978.

(41) Derbyshire, W.; Gorvin, T. C.; Warner, D. *Mol. Phys.* **1969**, *17*, 401.

(42) Hitchens, T. K.; Bryant, R. G. *J. Phys. Chem.* **1995**, *99*, 5612.

complexes as potential MRI contrast agents is a crucial point in determining proton relaxivity. For all the commercially available contrast agents, the proton relaxivity is limited by slow rotation of imaging fields. The order of τ_R values shown in Table 3, obtained from ^{17}O NMR spectroscopy or ^2H NMR, reflects the molecular size.

For the rotational correlation time, however, the simultaneous fit of ^{17}O NMR data, $1/T_1$, $1/T_2$, and ω yields a larger value than that obtained from only the ^2H NMR. The former ^{17}O NMR method has the drawback in measuring the τ_R of relying on distance estimates (the Gd–O distance), which have a strong influence on the absolute value of τ_R . The reason is that the Gd–water proton and Gd–water oxygen distances, used in the fit of the ^{17}O NMR data, are not known and, thus, can only be estimated. As a consequence, the absolute values of τ_R obtained from ^2H NMR and ^{17}O NMR can be different.

Binding Studies of Gd(III) Chelates to Human Serum Albumin (HSA). Binding of a Gd(III) complex to HSA is highly significant because the formed macromolecular adduct compared to the free complex results in a higher relaxivity and a longer retention time in the blood pool, which leads to a Gd(III) chelate for angiographic applications.²⁰ The characterization of the binding parameters consists of the determination of the enhancement factor ϵ^* through E and M titration.^{43,44} The former reports the change of ϵ^* as the concentration of HSA ratio increases, keeping $[\text{GdL}]_T$ constant. The fitting of these experimental data allows the evaluation of b and of the product $K_A \times n$ (K_A = association constant and n = number of independent sites). In the M titration, in contrast, the ϵ^* values are measured in solutions containing a fixed HSA concentration and variable concentration of Gd(III) complexes. The data from this titration are often more conveniently analyzed in the form of a Scatchard plot according to eq 5²⁰

$$r/[\text{GdL}]_F = nK_A - rK_A \quad (5)$$

where r represents the molar binding ratio, i.e., $[\text{GdL-HSA}]/[\text{HSA}]_T$ (where the T and F subscripts refer to “total” and “free” species, respectively). This ratio can be calculated when b is obtained from the E titration. In the case of a single class of binding sites, a plot of $r/[\text{GdL}]_F$ versus r gives a straight line whose x -axis intercept is equal to n , and whose slope corresponds to K_A . By assuming that the binding of successive molecules does not alter the K_A value of the bound complex, the curvature of a Scatchard plot implies that there is more than one class of binding sites, each one characterized by its own values of n , K_A , and b .

The results of the E and M titrations of the Gd(III) complexes with TTDA-BA and TTDA-MOBA are shown in Figures 5 and 6. The $[\text{Gd}(\text{TTDA-BA})(\text{H}_2\text{O})]^-$ and $[\text{Gd}(\text{TTDA-MOBA})(\text{H}_2\text{O})]^-$ complexes showed a significant increase in the longitudinal water proton relaxation rate

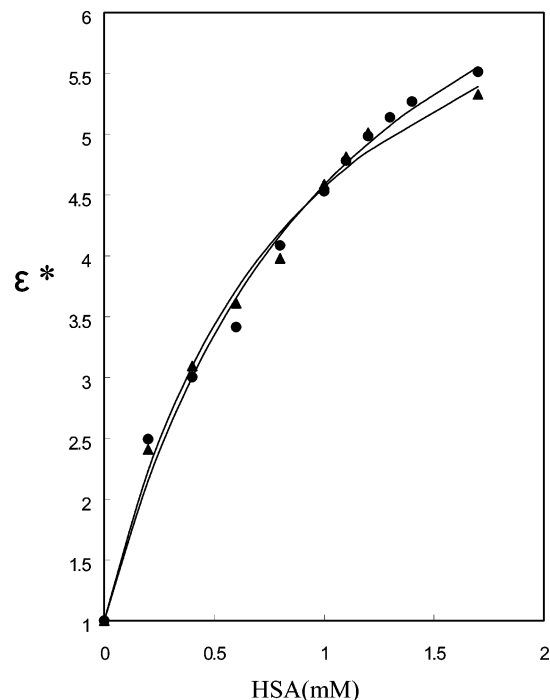


Figure 5. Plot of the water proton relaxation rate of the 0.1 mM $[\text{Gd}(\text{TTDA-BA})(\text{H}_2\text{O})]^-$ (●) and $[\text{Gd}(\text{TTDA-MOBA})(\text{H}_2\text{O})]^-$ (▲) solutions as a function of the HSA concentration (pH 7.5, 50 mM HEPES buffer, 20 MHz, 25 ± 0.1 °C).

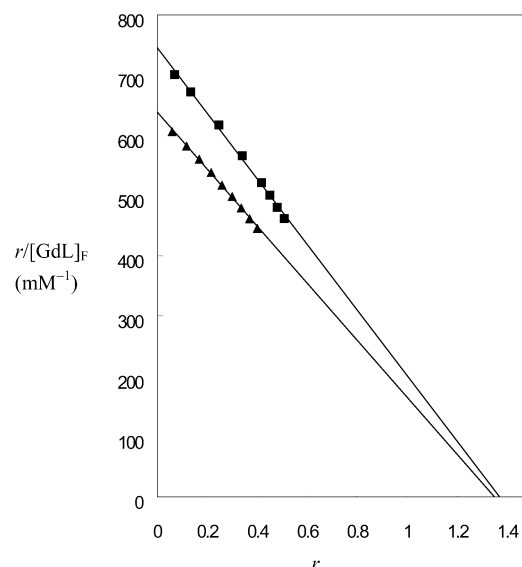


Figure 6. Scatchard plot of the data obtained from the PRE titration of a 0.6 mM HSA solution (pH 7.4, HEPES buffer, 25 ± 0.1 °C, 20 MHz) with $[\text{Gd}(\text{TTDA-BA})(\text{H}_2\text{O})]^-$ (▲) and $[\text{Gd}(\text{TTDA-MOBA})(\text{H}_2\text{O})]^-$ (■), $r = [\text{GdL-HSA}]/[\text{HSA}]_T$.

upon addition of HSA. The $[\text{Gd}(\text{TTDA-BA})(\text{H}_2\text{O})]^-$ and $[\text{Gd}(\text{TTDA-MOBA})(\text{H}_2\text{O})]^-$ complexes displayed the strongest interaction with HSA. The binding parameters calculated for the single strong binding sites to HSA of the two Gd(III) complexes are reported in Table 4. The K_A values of $[\text{Gd}(\text{TTDA-BA})(\text{H}_2\text{O})]^-$ and $[\text{Gd}(\text{TTDA-MOBA})(\text{H}_2\text{O})]^-$ are lower than that of MS-325⁴⁵ but are higher than that of $[\text{Gd}(\text{S-EOB-DTPA})]^{2-}$.⁴⁶ The affinity for HSA in this series

(43) Aime, S.; Botta, M.; Fasano, M.; Terreno, E. *Chem. Soc. Rev.* **1998**, 27, 19.

(44) Aime, S.; Botta, M.; Fasano, M.; Crich, S. G.; Terreno, E. *J. Biol. Inorg. Chem.* **1996**, 1, 312.

(45) Aime, S.; Chiaussa, M.; Digilio, G.; Gianolio, E.; Terreno, E. *J. Biol. Inorg. Chem.* **1999**, 4, 766.

Table 4. Binding Parameters to HSA from PRE Measurements (25 °C, 20 MHz, pH 7.4, 50 mM HEPES Buffer)^a

complexes	K_A (M ⁻¹)	n	r_1^F (mM ⁻¹ s ⁻¹)	r_1^{obs} (mM ⁻¹ s ⁻¹)	r_1^b (mM ⁻¹ s ⁻¹)	bound fraction
[Gd(TTDA-BA)] ⁻	$1.0 \pm 0.2 \times 10^3$	1	6.5 ± 0.3^b	21.9 ± 2.0	53.9 ± 2	36.9%
[Gd(TTDA-MOBA)] ⁻	$1.3 \pm 0.2 \times 10^3$	1	6.7 ± 0.2^b	21.3 ± 1.9	50.0 ± 1	42.1%
MS-325 ^c	$3.0 \pm 0.2 \times 10^4$	1	6.6 ± 0.4^b	42.0 ± 2.3	47.0 ± 4	52.5%
[Gd(S)-EOB-DTPA] ²⁻ ^d	$7.7 \pm 0.2 \times 10^2$	1	5.6 ± 0.4^b		44.1	

^a The relaxivity values for the bound chelates were calculated from solution containing 0.1 mM of the complexes and 4.5% of HSA. ^b These values are referred to solution containing 0.1 mM of paramagnetic complex in buffer. ^c Reference 47. ^d Reference 46.

of related Gd(III) complexes appears to be dependent on the hydrophobic substituents on the amide. The relaxivities of GdL–HSA adducts (r_1^b) were obtained by multiplying b by r_1^F . These values are remarkably high, and in particular in the case of [Gd(TTDA-BA)(H₂O)]⁻–HSA and [Gd(TTDA-MOBA)(H₂O)]⁻–HSA adducts, the obtained values of 53.9 and 50.0 mM⁻¹ s⁻¹ represent the higher relaxivity. The r_1^b values of [Gd(TTDA-BA)(H₂O)]⁻ and [Gd(TTDA-MOBA)(H₂O)]⁻ are slightly higher than those of MS-325 and [Gd(S)-EOB-DTPA]²⁻. Clearly, the bound relaxivity values of [Gd(TTDA-MOBA)(H₂O)]⁻ and [Gd(TTDA-MOBA)(H₂O)]⁻ are similar, indicating that the Gd(III) complexes may occupy similar positions on HSA.⁴⁷

Conclusions

The linear poly(aminocarboxylate) ligands, TTDA-MA, TTDA-BA, and TTDA-MOBA, form thermodynamically stable complexes with the trivalent Gd(III) ion. These complexes do not dissociate under physiological conditions (pH 7.4) and exchange with divalent Ca(II), Cu(II), or Zn(II) to an appreciable extent. The replacement of one carboxylate by an amide group decreases the water-exchange rate of Gd(III) complexes with TTDA-monoamide derivatives by a factor of about 5. From an analysis of the ¹⁷O NMR relaxometric properties, the replacement of a carboxylate with

an amide group and the introduction of a hydrophobic substituent on the amide group increases the lipophilicity of the Gd(III) complexes, therefore enhancing the relaxivity when it is bound to HSA. For small Gd(III) complexes such as those studied in this work, τ_R is the determinant correlation time at high fields and physiological temperature. An increased τ_R thus results in a higher relaxivity. [Gd(TTDA-MA)(H₂O)]⁻, [Gd(TTDA-BA)(H₂O)]⁻, and [Gd(TTDA-MOBA)(H₂O)]⁻ possess higher relaxivity, higher thermodynamic stability constants, and longer rotational correlation times and might result in a novel type of contrast agent for MRI. Moreover, the relatively strong binding between [Gd(TTDA-BA)(H₂O)]⁻ and [Gd(TTDA-MOBA)(H₂O)]⁻ and HSA increases the interest in its potential use as contrast agents for MR angiography. With the advantages of short τ_M and long τ_R of [Gd(TTDA-BA)(H₂O)]⁻ and [Gd(TTDA-MOBA)(H₂O)]⁻, more TTDA derivatives and their Gd(III) complexes are under development in our laboratory. We expect to obtain a novel contrast agent for MR angiography by tuning the lipophilicity of complexes with different hydrophobic substituent on the carbon backbone and pendant arm in the TTDA ligand.

Acknowledgment. We are grateful to the National Science Council of the Republic of China for financial support under Contract NSC 91-2113-M037-016.

Supporting Information Available: Additional figures, tables, and NMR details. This material is available free of charge via the Internet at <http://pubs.acs.org>.

IC049401W

(46) Vander Elst, L.; Chapele, F.; Laurent, S.; Muller, R. N. *J. Biol. Inorg. Chem.* **2001**, *6*, 193.

(47) McMurry, T. J.; Parmelee, D. J.; Sajiki, H.; Scott, D. M.; Ouellet, H. S.; Walovitch, R. C.; Tyeklár, Z.; Dumas, S.; Bernard, P.; Nadler, S.; Midelfort, K.; Greenfield, M.; Troughton, J.; Lauffer, R. B. *J. Med. Chem.* **2002**, *45*, 3465.